American Journal of Engineering Research (AJER) 2024
American Journal of Engineering Research (AJER)
e-ISSN: 2320-0847 p-ISSN : 2320-0936
Volume-13, Issue-5, pp-120-128
www.ajer.org
Research Paper Open Access

Millimeter Waves Reconfigurable antenna array using Compact Vivaldi source and Butler Matrix.

Amani CHERIF[1,2], Mohamed HIMDI[1], Xavier CASTEL[1], Saber DAKHLI[3], Fethi CHOUBANI[3]

[1]*Institut d'Electronique et des Technologies du numeRique (IETR), Université de Rennes, CNRS, IETR-UMR 6164, France*
[2]*Université de Tunis El Manar, Tunisia*
[3]*Innov'Com Laboratory LR11TIC03, SUPCOM, University of Carthage, Tunisia,*
Corresponding Author: mohamed.himdi@univ-rennes.fr

ABSTRACT: *The aim of this paper is to present a large bandwidth multi-beam antenna array in the millimeter wave range for 6G applications. The common source is a reconfigurable Vivaldi antenna that generates three beams (right, left, and front). The 4-element array is powered by a Butler matrix, originally producing 4 beams (2 on the right side and 2 on the left side). For the first time, we demonstrate that using a source with a reconfigurable radiation pattern allows for an extended coverage area greater than ± 115°, surpassing the capabilities of conventional methods.*

KEYWORDS *Butler matrix, Compact Vivaldi, Millimeter wave antenna arrays, large coverage.*

Date of Submission: 09-05-2024 Date of acceptance: 21-05-2024

I. INTRODUCTION

The rapid evolution of wireless communication technologies has driven the need for advanced antenna systems capable of meeting the demands of high data rates, low latency, and extensive coverage. In this context, reconfigurable antennas and Butler matrices [1] have emerged as crucial components in the design of next-generation communication systems, particularly for 6G applications.

Reconfigurable antennas [2,3] have gained significant attention due to their ability to dynamically alter their radiation pattern, polarization, frequency, and directivity [4]. This adaptability makes them ideal for various applications, from mobile communications to radar systems and satellite communications. By incorporating active components such as RF switches, varactors, or MEMS devices, reconfigurable antennas can change their configuration in real-time, thus optimizing performance for different operating conditions and requirements.

One of the primary advantages of reconfigurable antennas [5,6] is their potential to enhance system capacity and coverage. For instance, a reconfigurable Vivaldi antenna can switch between different beam patterns, providing broadside, left, and right beams, thus covering a wider area compared to conventional fixed-beam antennas. This flexibility is particularly beneficial in millimeter-wave (mmWave) frequencies [7], where signal attenuation and propagation challenges are more pronounced.

Complementing reconfigurable antennas, the Butler matrix is a key technology used to achieve multiple beamforming [8-11]. A Butler matrix is a type of beamforming network that uses a combination of hybrids, phase shifters, and crossover devices to create multiple fixed beams from a single antenna array. This capability makes Butler matrices essential for applications requiring high directivity and multiple beam generation, such as in phased array systems and MIMO (Multiple Input Multiple Output) configurations.

The integration of reconfigurable antennas with Butler matrices offers significant benefits for 6G applications. By combining the dynamic beamforming capabilities of reconfigurable antennas with the multi-beam generation of Butler matrices, it is possible to achieve enhanced coverage, increased capacity, and improved signal quality. This paper explores the design and implementation of a high-bandwidth multi-beam antenna array using a reconfigurable Vivaldi antenna and a Butler matrix. The proposed system demonstrates extended coverage and superior performance compared to traditional methods, marking a significant advancement in antenna technology for future wireless communication networks.

II. ANTENNA DESIGN

The proposed reconfigurable wideband Vivaldi antenna was fabricated on a 25.4 mm × 25.4 mm × 0.5 mm fused quartz substrate, featuring a dielectric permittivity of εr = 3.75 and a loss tangent of tan = 4×10^{-4} at 25 GHz. The antenna includes a 7.25 mm × 8.94 mm radiating element composed of two distinct parts, referred to as petals, along with a uniquely shaped ground plane printed on the front side of the substrate (Fig. 1a). The radiating element is powered by a slot/microstrip line transition, utilizing a 3.1 mm-wide microstrip line ending in a 0.6 mm-radius quarter circle printed on the rear side of the fused quartz substrate (Fig. 1b). On the front side of the substrate, three PIN diodes could be integrated onto the tapered slot lines to enable reconfigurable radiation patterns (Fig. 1a). The slot line along the y-axis terminates in a 0.22 mm-radius circular slot (Fig. 1b).

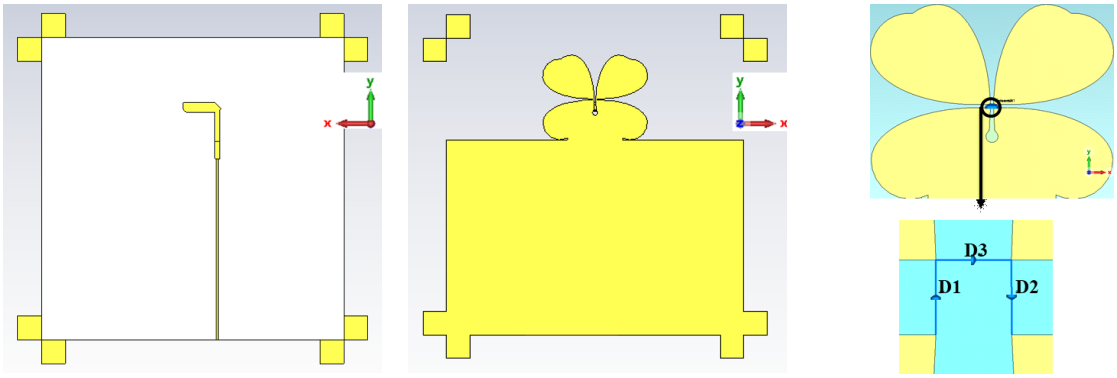

a) b) c)

Fig. 1. The Vivaldi antenna in: front side (a) rear side (b) and zoom of the three PIN diodes.

PIN diodes, labeled D1, D2, and D3, manage the reconfiguration of the slots to enable three distinct states of operation. In state 1, D1 and D2 are in the ON state (acting as short-circuits), while D3 is in the OFF state (acting as an open circuit). In state 2, D2 and D3 are ON, and D1 is OFF. In state 3, D1 and D3 are ON, and D2 is OFF. These configurations are summarized in Table I.

Modes	Diodes state		
	D1	*D2*	*D3*
State 1	ON	ON	OFF
State 2	OFF	ON	ON
State 3	ON	OFF	ON

Table 1. Operating states

Fig. 2 shows the simulation of the S-parameter for of antenna on state 1. It is noteworthy that it exhibits a wide bandwidth, ranging from 23 to 31 GHz, with $|S_{11}|$ values below -10 dB. This indicates that the antenna effectively covers the 5G millimeter-wave band. The other states are very similar.

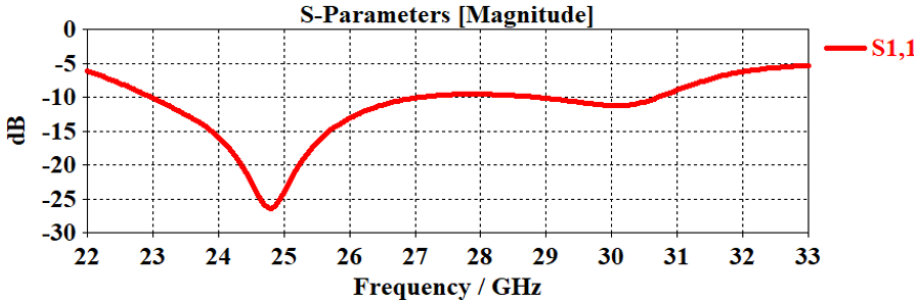

Fig. 2. Simulated S11 of the Vivaldi antenna fabricated on a 0.5 mm thick quartz substrate for state 1.

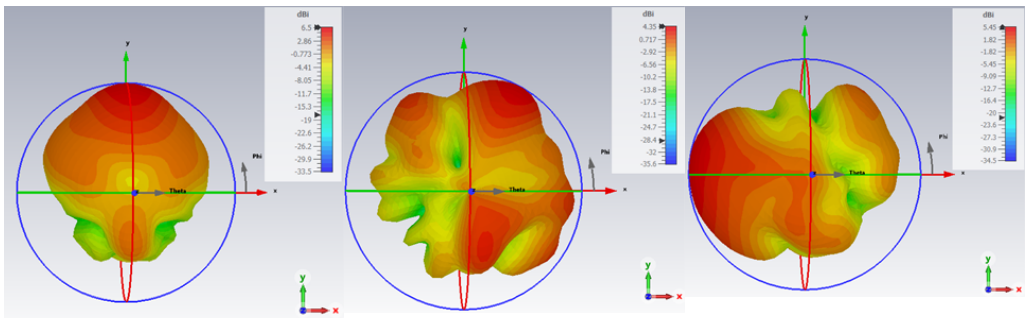

a) **b)** **c)**

Fig.3. 3D radiation pattern of Printed Vivaldi antenna at 26.5 GHz for state 1 (a); state 2 (b); state 3 (c)

The radiation beam can be manipulated by directing the current flow through D1, D2, or D3 PIN diodes. In state 1, with D1 and D2 in the ON state, the beam radiates along $\phi = 90°$ (Fig. a). State 2 exhibits current deviation on the right side of the tapered slot (Fig. 3b), while state 3 shows this deviation on the left side (Fig. 3c). Thus, the Vivaldi antenna's radiation pattern can be adjusted across a 300° ϕ angle using these three states.
A peak gain of 6.5 dBi is observed at 26.5 GHz for state 1 (Fig. 4), while the peak gain reach 7.5 dBi at 29 GHz

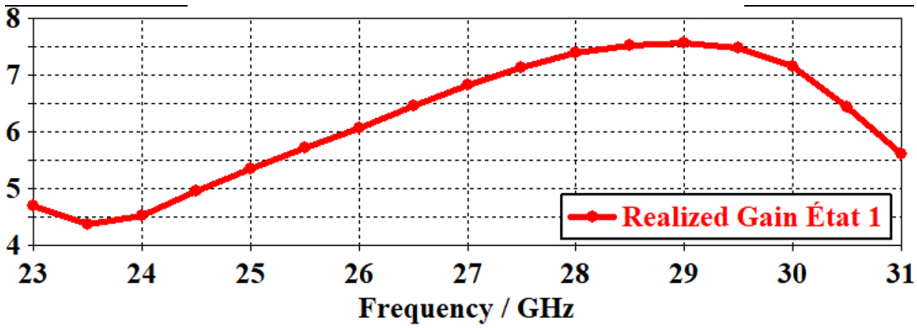

Fig.4. Simulated gain (dBi) of the Vivaldi antenna on state 1.

Fig. 4 shows the gain (dBi) of this antenna in state 1 as a function of frequency, with an average reaching 6 dBi. The primary goal is to integrate this source into a 4-element array, feeding it through a Butler matrix, and exploring various combinations of source states.

III. BUTLETR MATRIX DESIGN

Interest in Butler matrix theory, originating in the 1960s, continues to grow due to its applications in beamforming networks for multibeam antennas, both active and passive. A Butler matrix is a passive circuit with \(N\) input ports and \(N\) output ports, designed to control \(N\) radiating elements to produce \(N\) distinct orthogonal beams. The number of beams generated by a Butler matrix corresponds to its number of input ports (\(N\)). The various stages of power division, consisting of couplers and phase shifters, define the phases needed to steer the array of \(N\) elements in the desired directions.

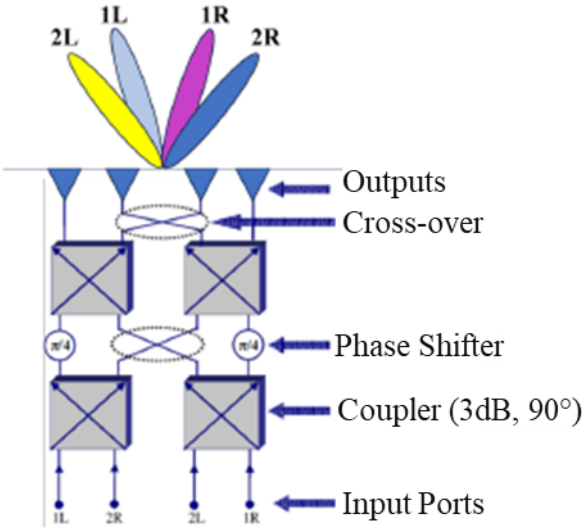

Fig. 5. Butler Matrix Configuration for 4-Element Antenna Array Beamforming

The network combines these signals through 4 distinct channels to generate a beam in a direction given. Each input corresponds to outputs with phase spacing regular, which drives a beam in a specific direction. The unpointing of these 4 beams is determined by the formula:

$$\phi_m = \sin(\theta_m).\ 2\pi d/\lambda_0 \cdot \qquad (1)$$

Where: ϕ_m: phase gradient between two consecutive radiating elements
d: distance between radiating elements
λ_0: wavelength in air
θ_m: angle made by the beam m with the normal to the antenna array
We note that the tilt angle of a beam θ_m is effectively influenced by the distance d between the elementary antennas. The proposed Butler Matrix (BM) was designed completely from the conventional couplers and Crossovers designed using commercially available Computer Simulation Technology (CST).

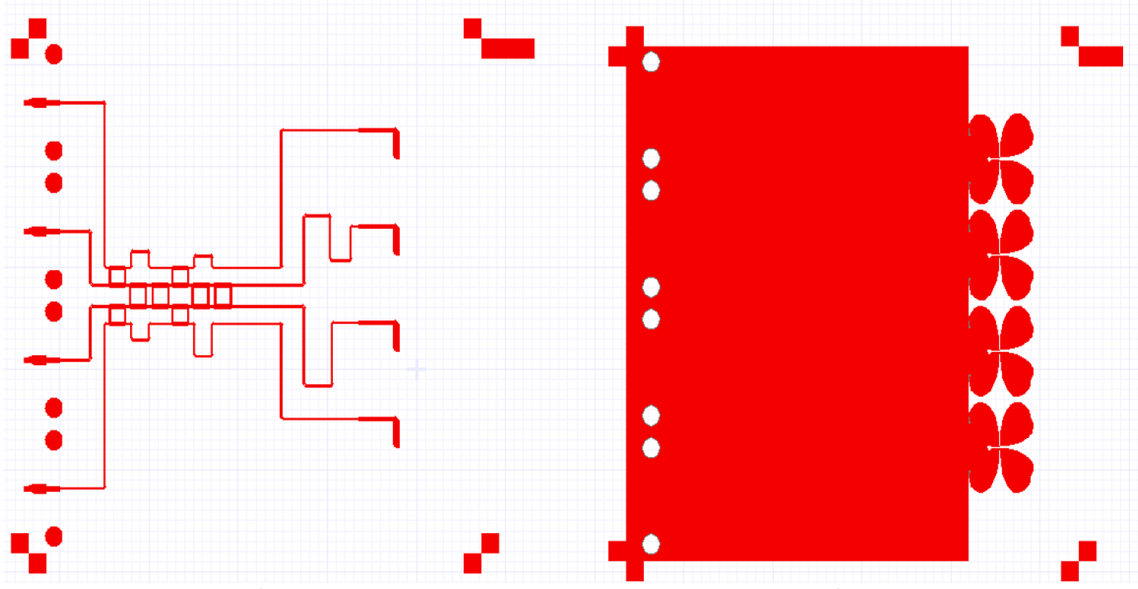

a) **b)**

Fig. 6. layout design for a 4-element antenna array fed by a Butler matrix. Front side (a) rear side (b).
Fig. 6 depicts a layout design for a 4-element antenna array fed by a Butler matrix. Let's break down the components:

1. **Left Side (Butler Matrix):** The intricate network of lines and intersections represents the Butler matrix, which is a type of beamforming network. It consists of several couplers and phase shifters to provide the necessary phase differences to each antenna element.
2. **Right Side (Antenna Array):** The array on the right shows four Vivaldi radiating elements. These are connected to the Butler matrix outputs.

Components:

- **Butler Matrix:**
  - **Couplers:** These are used to split and combine signals with specific phase shifts.
  - **Crossovers:** Used to maintain the layout of the matrix while routing signals.
  - **Phase Shifters:** These introduce the required phase shifts to create different beam directions.
- **Antenna Elements:**
  - **Array Configuration:** The elements are arranged in a linear fashion to form a phased array. The spacing between antenna elements should be optimized to prevent grating lobes and ensure effective beam steering. In our case, $0.79\lambda_0$ is used at 25 GHz.
  - **Feed Points:** The connections from the Butler matrix to the antennas use microstrip/sot line transition.

Functionality:

The Butler matrix provides a means to control the direction of the antenna beam without mechanical movement. By switching between different input ports, the matrix creates different phase shift combinations, steering the beam in various directions.

We start by using the element Vivaldi antenna in the state 1. That correspond to classical configuration. In this case with the choosing distance $d=0.79\lambda_0$ at 25 GHz, we obtain 4 beams at ± 9° and ± 29°. The fig. 7 confirms these theoretical results.

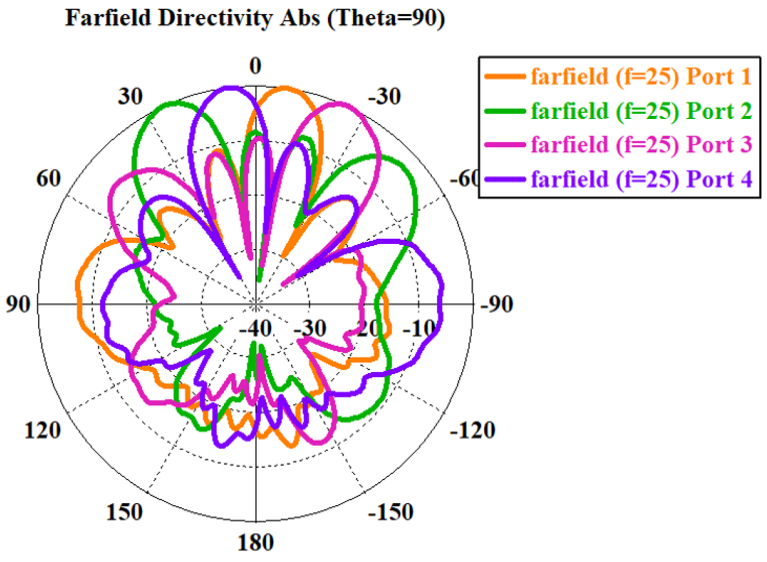

Fig. 7. Radiation Patterns at Theta = 90° for a 4-Element in state 1 Antenna Array Fed by a Butler Matrix

This fig. 7 polar plot illustrates the farfield directivity patterns (in dB) at Theta = 90° for a 4-element antenna array. Each curve corresponds to the excitation of a different input port of the Butler matrix at a frequency of 25 GHz.

The plot fig. 7 demonstrates how the Butler matrix creates distinct orthogonal beams for each input port, achieving beamforming and direction control for the antenna array. The radial axis represents the directivity in decibels (dB), while the angular axis (Phi) is in degrees.

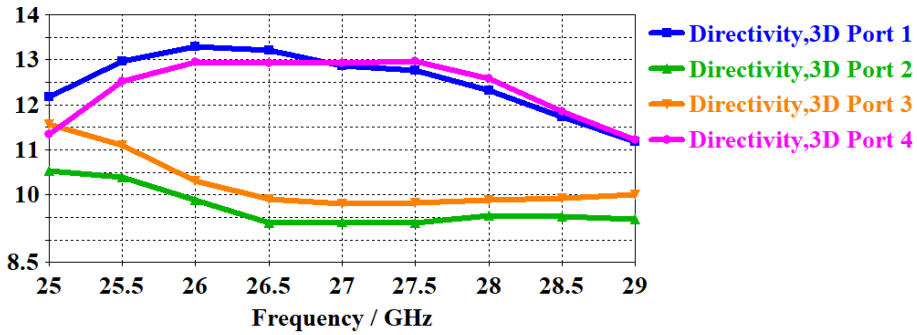

Fig. 8. 3D max Directivity versus frequency for a 4-Element in state 1 Antenna Array Fed by a Butler Matrix

This graph fig. 8 shows the frequency response of the 3D directivity (in dBi) for each port of a 4-element antenna array fed by a Butler matrix, over a frequency range of 25 GHz to 29 GHz. Each colored line represents the directivity performance of a specific port across the given frequency band.

The proposed compact and reconfigurable Vivaldi antenna can operate in two additional states, 2 and 3. This section aims to explore the behavior of the array using these alternative element states while maintaining the same Butler matrix design.

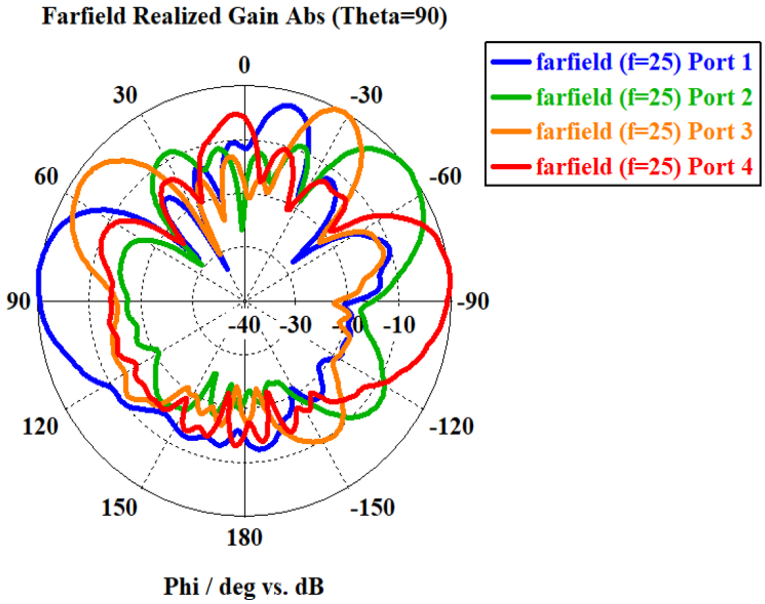

Fig. 9. Radiation Patterns at Theta = 90° for a 4-Element in state 2 Antenna Array Fed by a Butler Matrix

This fig. 9 polar plot illustrates the farfield directivity patterns (in dB) at Theta = 90° for a 4-element antenna array. Each curve corresponds to the excitation of a different input port of the Butler matrix at a frequency of 25 GHz. We can observe that this configuration enables coverage of additional areas, producing new beams at -50°, -75°, and +80°. The plot fig. 9 demonstrates how the Butler matrix creates distinct orthogonal beams for each input port, achieving beamforming and direction control for the antenna array. The radial axis represents the directivity in decibels (dB), while the angular axis (Phi) is in degrees.

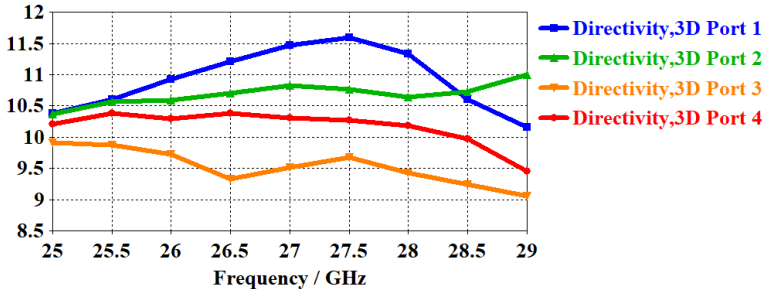

Fig. 10. 3D max Directivity versus frequency for a 4-Element in state 2 Antenna Array Fed by a Butler Matrix

This graph fig. 10 shows the frequency response of the 3D directivity (in dBi) for each port of a 4-element antenna array fed by a Butler matrix, over a frequency range of 25 GHz to 29 GHz. Each colored line represents the directivity performance of a specific port across the given frequency band.

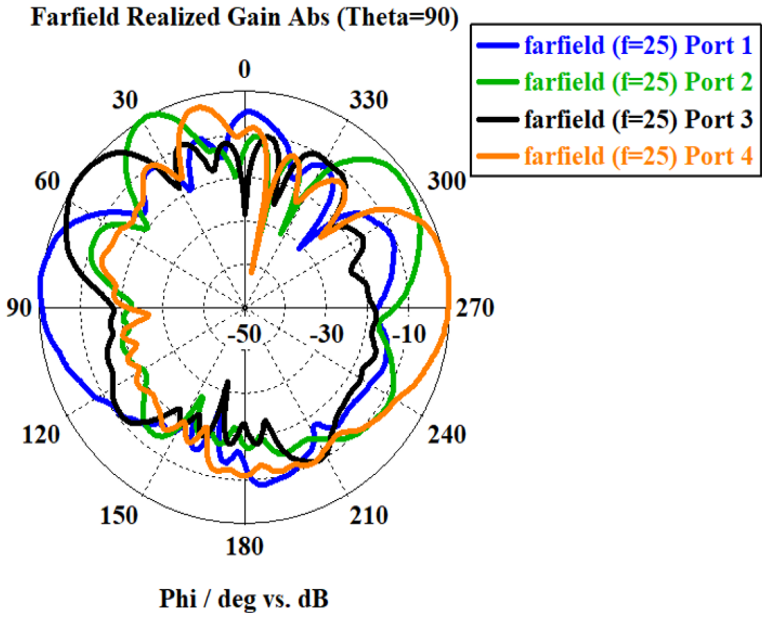

Fig. 11. Radiation Patterns at Theta = 90° for a 4-Element in state 3 Antenna Array Fed by a Butler Matrix

This fig. 11 polar plot illustrates the farfield directivity patterns (in dB) at Theta = 90° for a 4-element antenna array. Each curve corresponds to the excitation of a different input port of the Butler matrix at a frequency of 25 GHz. We can observe that this configuration enables coverage of additional areas, producing new beams at +50°, +75°, and -80°.

The plot fig. 11 demonstrates how the Butler matrix creates distinct orthogonal beams for each input port, achieving beamforming and direction control for the antenna array. The radial axis represents the directivity in decibels (dB), while the angular axis (Phi) is in degrees.

This graph fig. 12 shows the frequency response of the 3D directivity (in dBi) for each port of a 4-element antenna array fed by a Butler matrix, over a frequency range of 25 GHz to 29 GHz. Each colored line represents the directivity performance of a specific port across the given frequency band.

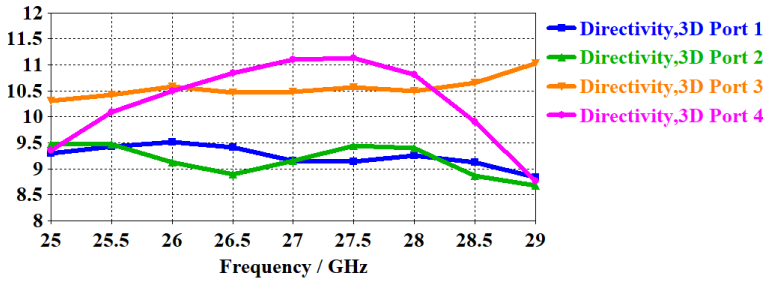

Fig. 12. 3D max Directivity versus frequency for a 4-Element in state 3 Antenna Array Fed by a Butler Matrix

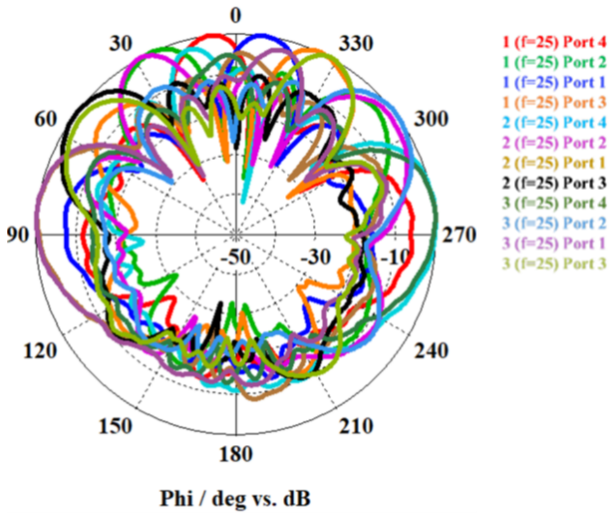

Fig. 13. Radiation Patterns at Theta = 90° for a 4-Element in all states Antenna Array Fed by the same Butler Matrix

This fig. 13 polar plot illustrates the farfield realized gain patterns (in dB) for a 4-element antenna array fed by a Butler matrix, showing the performance across different states (1, 2, and 3) and ports at a frequency of 25 GHz: We can observe that the total coverage of additional areas extends to approximately ±115°.

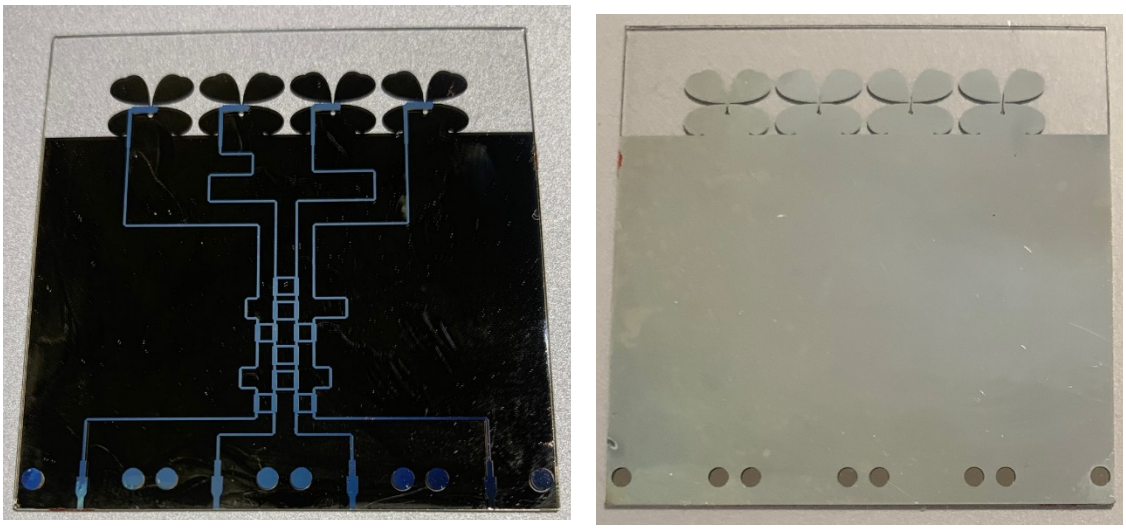

a) **b)**

Fig. 14. Fabricated 4-Element Antenna Array with Butler Matrix Feed Network. Front side (a) rear side (b).

This image shows a photolithography fabricated 4-element antenna array integrated with a Butler matrix feed network on a transparent quartz substrate. Key features include:

Input Ports: The top section shows the input ports where signals are fed into the Butler matrix.
Butler Matrix: The intricate network in the center consists of couplers, phase shifters, and crossovers, forming the Butler matrix. This network distributes signals to the antenna elements with the appropriate phase shifts.
Antenna Elements: The bottom section displays four distinct antenna elements, likely Vivaldi antennas, arranged linearly.
This setup is used to demonstrate beamforming capabilities and the creation of multiple distinct beams for improved coverage and directivity. Measurements of the prototype are currently underway.

IV. CONCLUSION

In this paper, we presented a compact and reconfigurable Vivaldi antenna array integrated with a Butler matrix, designed for millimeter-wave applications pertinent to 6G technology. The integration of a reconfigurable antenna with a Butler matrix enables the generation of multiple distinct beams, thereby significantly enhancing coverage and beamforming capabilities. The fabricated prototype demonstrated the ability to switch between three different states, each providing unique radiation patterns. State 1 produced beams at ±9° and ±29°, while States 2 and 3 allowed for additional coverage at angles such as -50°, -75°, and +80°. The overall coverage area achieved with this setup extends to approximately ±115°, which surpasses the performance of conventional fixed-beam antenna systems. Simulation and preliminary measurement results confirmed the effectiveness of this design, showing promising directivity and gain across a wide frequency range from 25 GHz to 29 GHz. These results validate the proposed system's potential for high-data-rate, low-latency communication in future wireless networks.

Further work will focus on the complete characterization of the prototype and optimization of its performance in practical scenarios. This advancement marks a significant step towards the development of versatile, high-performance antennas for next-generation communication systems.

ACKNOWLEDGMENTS

This work is supported by the European Union through the European Regional Development Fund (ERDF), the Ministry of Higher Education and Research, the Région Bretagne, the Département des Côtes d'Armor and Saint-Brieuc Armor Agglomération, through the CPER Projects 2015-2020 MATECOM and SOPHIE/STIC & Ondes.

REFERENCES

[1]. J. Butler and al., "Beam-forming matrix simplifies design of electrically scanned antennas", Electronic Design, vol. 9, pp.170 -173, Apr. 1961.
[2]. F. Yang and Y. Rahmat-Samii, "Reconfigurable Antennas," in IEEE Transactions on Antennas and Propagation, vol. 54, no. 3, pp. 556-568, March 2006.
[3]. J. T. Bernhard, "Reconfigurable Antennas," in Reconfigurable Antennas, San Rafael, CA: Morgan & Claypool, 2007.
[4]. R. J. Mailloux, "Phased Array Antenna Handbook," 2nd ed., Norwood, MA: Artech House, 2005.
[5]. M. Bozzi, S. Germani, and L. Perregrini, "Performance of Vivaldi Antennas With Reconfigurable Radiation Pattern," IEEE Antennas and Wireless Propagation Letters, vol. 3, pp. 183-186, 2004.
[6]. A. Cherif, M. Himdi, X. Castel, Q. Simon, S. Dakhli, F. Choubani,"Radiation Beam Width and Beam Direction Electronic Control of Transparent and Compact Vivaldi Antennas", Applied Sciences, Special Issue in Advanced Infrared Semiconductor Lasers and Integrated Optics Devices., Appl. Sci. 2023, 13, 7878. doi.org/10.3390/.
[7]. T. S. Rappaport et al., "Millimeter Wave Mobile Communications for 5G Cellular: It Will Work!" in IEEE Access, vol. 1, pp. 335-349, 2013.
[8]. M. Li, K. M. Luk, and C. H. Chan, "A Butler Matrix-Based Design for Multi-Beam MIMO Antennas," in IEEE Transactions on Antennas and Propagation, vol. 62, no. 2, pp. 621-628, Feb. 2014.
[9]. 0. Lafond, M. Himdi, J.P. Daniel, "Thick slot coupled printed antennas arrays for a 60 GHz indoor communication system", Microwave and Optical Technology Letters, Vol. 25, No. 2, pp. 105-108, 20th January 2001.
[10]. S. A. Babale, A. R. Sharul, O. A. Barro, M. Himdi, M. Khalily, "Single Layered 4 x 4 Butler Matrix Without Phase-shifters and Crossovers", IEEE Access, Vol. 6, Issue 1, Pages: 77289-77298, December 2018.
[11]. M. K. Ishfaq, S. A Babale, H. T. Chattha, M. Himdi, A. Raza, M. Younas, T. A. Rahman, S. K. A. Rahim, B. A. Khawaja, "Compact Wide-Angle Scanning Multibeam Antenna Array for V2X Communications", IEEE Antennas and Wireless Propagation Letters, vol. 20, no. 11, pp. 2141-2145, Nov. 2021, doi: 10.1109/LAWP.2021.3100349